A Study on Design Methodologies for Compact Electric Machines Used in Electrified Mobile Hydraulics

Parth Tawarawala[1,*], Shanmukh Sarode[1], Hassan Assaf[1], Andrea Vacca[1], Lizhi Shang[1] and Scott D. Sudhoff[2]

[1]*Maha Fluid Power Research Centre, Purdue University, West Lafayette, Indiana, USA*
[2]*Elmore Family School of Electrical and Computer Engineering, Purdue University, West Lafayette, Indiana, USA*
E-mail: ptawaraw@purdue.edu
[*]*Corresponding Author*

Received 06 February 2024; Accepted 26 June 2024

Abstract

Electric Machines (EMs) have gained increasing importance in the mobile hydraulic industry as prime movers for hydraulic actuation systems. Therefore, their design and sizing are important aspects for any system layout architecture. The on-road vehicle industry has exploited EM versatility by proposing different sizes for various applications. However, off-road vehicles cannot borrow designs from on-road applications directly due to their unique challenges pertaining to drive cycle dynamics and limited space availability. Furthermore, considerations of the thermal limitations of EM and their cooling must also be studied to devise an effective methodology for designing prime movers suitable for mobile hydraulic applications.

This paper proposes EM operational sizing strategies based on corner point operation, flux weakening and transient operation that can downsize EMs by carefully selecting sizing points from the operating domain. These strategies can leverage the operational capabilities of EMs and involve trade-offs in terms of EM compactness and efficiency. Therefore, based on a

International Journal of Fluid Power, Vol. 25_3, 375–412.
doi: 10.13052/ijfp1439-9776.2534

specific requirement, a given strategy can have certain benefits explored in this paper. The paper also examines two other downsizing methods based on switching the ePump architecture to variable displacement pump operation and improving the cooling performance. The paper considers a 5-ton mini excavator's arm actuator as a reference application. The resulting EMs are compared in terms of size and efficiency to study the effectiveness of each operational sizing strategy. This paper uses a well-established genetic algorithm-based multi-objective algorithm to design a Permanent Magnet Synchronous Machine (PMSM) for each sizing strategy. The effect of cooling technology is considered in terms of limiting winding current density for the EMs, and the impact of cooling technology on the size and efficiency of the EM is also demonstrated. Finally, the effectiveness of the proposed operational sizing strategies in downsizing EMs is combined with, and compared to other methods like variable displacement operation and aggressive cooling to identify the best ways to obtain the most compact EMs for any hydraulic application.

Keywords: Electrification, operational sizing, electric machine optimization, off-road vehicles, cooling technology, ePump.

1 Introduction

With global efforts on emission reduction and elimination of fossil fuels underway, the off-road vehicle (ORV) industry is witnessing major changes, with efforts on alternative prime mover technologies particularly gaining momentum in academia and industry alike. One such technology is given by the use of Electric Machine (EM) in fully electric or hybrid-electric vehicles, which can drive the hydraulic supply systems that performs the hydraulic actuations in the vehicle. Therefore, the study of the design of EMs and their specific applicability to mobile fluid power systems is a topic of ongoing research and is also the focus of the current paper.

Electric Machines can suffer from multiple shortcomings. Their cost and reliance on rare earth materials can make them a hindrance to OEMs. Their power density can also be a major concern for mobile applications, where the space of ORVs can be limited. As shown by Sayako et al. [1], EMs have inherently lower power densities than hydraulic technologies. This makes the EM size a determining factor for their application in ORVs. Another primary consideration for EMs is their thermal management. Electric Machine operation can involve a large amount of heat generation inside stator windings,

which can damage the EM if not properly managed. Therefore, focus must be placed on designing effective cooling technology for EMs used in ORVs to maximize productivity and decrease operational costs.

Electric Machines also offer a unique set of benefits, making them particularly well-suited for fluid power systems. One of their benefits includes the possibility of using a decentralized fluid power system. Such systems eliminate a significant portion of throttling losses, increasing the operating efficiency of the entire system. Furthermore, the ability to control the EM speed in flow control applications allows for the use of cheaper fixed displacement pumps or can allow for variable displacement pumps to operate at their maximum efficiency.

One such type of Electric Machine architecture of interest is the Permanent Magnet Synchronous Machine (PMSM). These EM architectures are preferred in electrification applications due to their superior efficiency and power density, as reported by [2] and [3] in their study on on-road vehicles. The versatility of PMSMs means that they can be effectively incorporated in ORVs, as can be seen in several state-of-the-art works, like [4, 5], and [6]. This also means that the design strategies for PMSMs in on-road vehicles can be applied to ORVs as well, and therefore, the authors focus on PMSM design for this paper.

EMs like PMSM can operate in multiple operational modes [7], like flux weakening and overload conditions, a feature that can be used to downsize these machines based on a specific operating requirement. A flux weakening-based operating strategy was proposed by Sudhoff et al. [8] to extend the operating speed of a surface-mounted PMSM. Such a flux weakening-based operational sizing strategy was also employed by the authors' lab for fluid power systems in [9] to drive an axial piston pump. Another important operating characteristic for PMSMs that can be leveraged is overload operation. This strategy involves designing the PMSM for sustained operation in the continuous operation domain while also allowing the EM to operate in overload conditions for a short time, taking thermal constraints into account. This strategy can downsize the EM significantly, compared to studies where EMs are designed for sustained operation for all operating points in the drive cycle, like in [10] and [11]. Such a strategy was demonstrated by Pellegrino [12], where the authors had used an overload current equal to 173% of the rated value to design a surface-mounted and internal PMSM. This implies that the motors designed in the study could yield a maximum overload torque that was 1.73 times the rated torque in the torque per amp mode. Even for commercial PMSMs, like Parker Hannifin's [13], it can be seen that the overload current

can be as much as 1.7-2.1 times the rated current. Authors in [12] and [14] also showed how the overload capability for PMSMs can be exploited for use in urban EV applications. Gamba [14] used a sizing torque based on RMS values of instantaneous values in a time window, which was 33% of the maximum torque required in the drive cycle.

These operating modes have a significant potential for application in mobile hydraulic machines, where downsizing the EMs would make their installation easier, further boosting the industry's electrification efforts and decreasing the enormous gap between power densities of electric and hydraulic technologies.

In addition, decentralized systems with variable displacement hydraulic units open up new possibilities to increase the efficiency of the entire system, as demonstrated in [15]. The speed of the EM and the displacement of the HM can both be simultaneously adjusted such that the combined unit always operates at maximum efficiency while meeting the flow demand of the hydraulic actuation system. Furthermore, lowering the displacement can reduce the bleed-off losses in very low flow demands, as shown in [16]. Lowering the displacement has another benefit in reducing the torque demanded by the HM, allowing further downsizing of the EM. This performance comparison on ePump architectures for mobile applications was also done in [17].

To explore all the possibilities mentioned above, a methodology to design optimal EMs must also be considered. EM design can be a complex problem, as it involves consideration of geometry, materials, and winding distribution. Algorithms for quick computation of EM performance are often embedded inside multi-objective optimization strategies to design EMs that can satisfactorily meet any application demand. An example of this can be seen in Nishanth [4]. The EM design strategy used for the current paper has been devised by Sudhoff [18, 19] and is described in further sections. The selected design strategy can be used to design an EM while minimizing size and power loss for a chosen fluid power application based on operating points derived from the above-mentioned operating strategies.

Therefore, the objective of the current research is to propose and comprehensively compare different EM operational sizing strategies, those being corner point operation, flux weakening operation and transient operation, for two different ePump architectures and design an EM to drive the hydraulic supply of an ORV. Section 2 will describe the reference application in detail, followed by a brief description of the considered ePump architectures. Section 3 will then describe the EM optimization algorithm and the proposed operational sizing strategies that can be used for the given applications,

followed by results in Section 4 that compare the resulting EMs in terms of size and efficiency. Given the importance of thermal management in EMs, an analysis will also be conducted to show the effect of different cooling technology on the EM sizing strategies in Section 5. Lastly, the effectiveness of the proposed operational sizing strategies when compared to, or in combination with, other downsizing methods, like switching ePump architectures or improving the cooling technology, will be demonstrated in Section 6. The current paper represents and extension of the work of the SICFP 2023 paper [19], it essentially repeats Sections 1–4 for completeness, while Sections 5–7 are the novel contribution of the extended journal publication

2 Reference Application Description

The reference mobile hydraulic machine considered for the current study is a 5-ton mini excavator. One such machine is present at the authors' research lab and is shown in Figure 1, with labels corresponding to each of the main actuators: boom, arm, bucket and swing. While a mini-excavator can perform many functions, a very common one is the digging and loading cycle, also considered in the current study. The baseline hydraulic architecture for the reference machine is a post-compensated load-sensing (LS) system. In previous works at the author's lab [21, 22] a decentralized Displacement-Control (DC) hydraulic system was implemented and compared to the baseline LS system for the same working cycle. The study demonstrated how a decentralized hydraulic actuation could bring energy efficiency gains up to 40% with respect to the conventional centralized system. It also showed that among the main actuators, the arm of the machine experiences the highest dynamics, making its design challenging for electrification applications. Therefore, the authors selected the arm actuator for their study on electrification, considering a highly efficient actuation system with all functions as individual systems.

For the current study, two different architectures for ePumps are considered (Figure 2) based on flow control strategy: one where the EM has a variable speed that can be achieved by the use of an inverter and the pump has a fixed displacement (VMFP) and one where the motor speed is fixed, and the pump displacement is varied (FMVP), by means of hydraulic or electro-hydraulic control architectures. The third type of ePump architecture, based on VMVP operation, where both EM speed and HM displacement are varied and chosen to maximize efficiency, is outside the scope of the current paper.

The pump power, flow and pressure supply for the chosen actuator drive cycle are shown in Figure 3. The high dynamics present in the system can

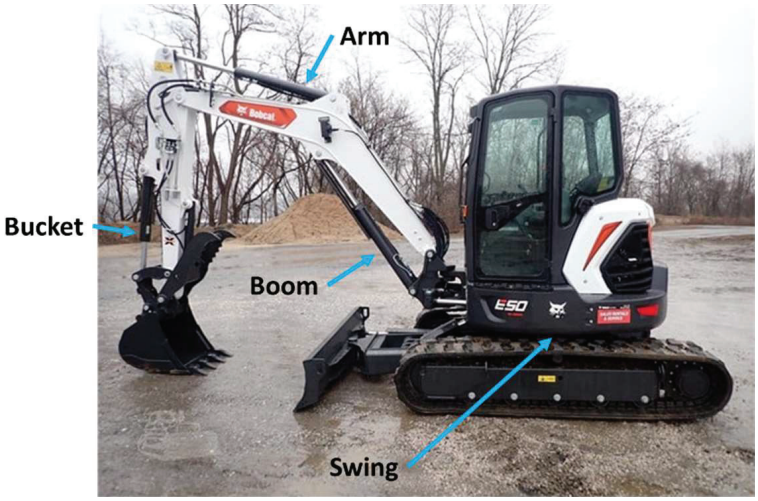

Figure 1 5-ton mini excavator used as reference machine.

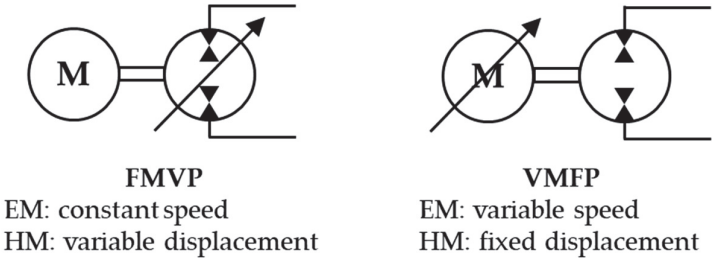

Figure 2 Architectures considered for ePumps: (a) FMVP and (b) VMFP.

be observed in these plots. One notable aspect of the currently shown drive cycle is the absence of overrunning loads. It is assumed that overrunning loads are handled with a meter-out orifice that prevents the load from falling and allows the actuator to reach the desired velocity. This implies that the system always operates in the first quadrant and does not recover energy. This consideration is made because recovering energy requires expensive components, like a battery or an over-centre pump. Furthermore, specifically looking at the arm actuator, the recoverable energy is much lower than other excavator actuators like boom and swing [23]. Therefore, limiting the analysis to the 1st quadrant is a reasonable assumption.

To meet the maximum pressure and flow requirements, an HM is sized, which can work for both ePump architectures. The HM selected is an 18

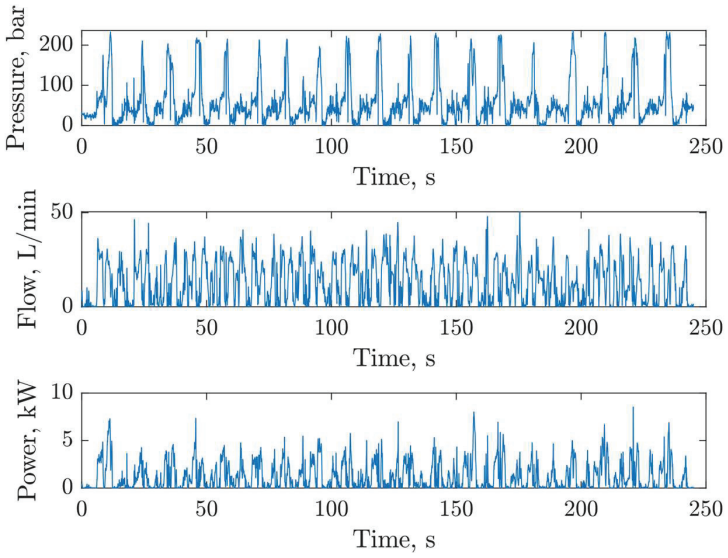

Figure 3 Pressure, Flow and Power drive cycle for the selected actuator.

cc/rev Axial Piston Machine available at the authors' lab that can reach a maximum speed of 3000 RPM.

3 Electric Machine Design

Before a design procedure for EMs can be laid out, it is important to select an EM type that can be suitable for the current application. There exist multiple types of EMs, each having its own strengths. Induction Machines are known for their low cost and simple design, but can suffer from low efficiency and power density, widening the gap between power densities of hydraulic and electric machines. Permanent Magnet Synchronous Machines (PMSMs) perform much better, in terms of efficiency and size [3], and therefore, their adoption in fluid power applications has also been studied widely in literature [4, 10, 11]. Among PMSMs, two categories of EMs exist: Internal Permanent Magnet Motor (IPM) and Surface-mounted Permanent Magnet Synchronous Machine (SPMSM). Based on the authors' observations in a previous study [17], SPMSMs can handle overload torques much better than IPMs, making them particularly attractive for systems with high dynamics, like in fluid power, and therefore, SPMSM has been selected for the current study.

Multiple design methodologies exist for the analysis and design of PMSMs that can meet any requirement. The analysis methodology selected in the current study is based on a lumped parameter-based Magnetic Equivalent Circuit (MEC) model of a current-controlled, 3-phase, wye-connected Surface Mounted Permanent Magnet Synchronous Machine (PMSM), as described in [18]. This formulation allows for a very fast evaluation of the winding and field parameters of a particular design configuration. This MEC-based model is then embedded inside a non-sorting Genetic Algorithm (NSGA-II) tool [19] that minimizes two objective functions: motor size and motor power loss for a given set of operating points. This section will briefly describe the optimization structure used for designing EMs in the study for completeness, however, readers interested in a more in-depth understanding of the optimization formulation are referred to [18].

For the quantification of overall EM fitness, 2 objective functions are used:

1. EM Size
2. EM Power loss

The EM size is defined as the geometric mean of motor mass and volume, as given by (1). This parameter is defined, instead of using the EM mass or volume directly, to ensure that the pareto-optimal front is not heavily biased towards one of these parameters. For example, using only mass as an objective function may yield EM designs that are lightweight, but occupy a lot of volume, making them unsuitable for installation on an ORV, and vice versa. Therefore, combining both mass and volume to define EM size ensures that minimization of this parameter yields EMs that have both high specific and volumetric power densities. The units of size are therefore $(kg - L)^{\frac{1}{2}}$

$$S_{EM} = (M_{EM} \times V_{EM})^{\frac{1}{2}} \tag{1}$$

The EM power loss is composed of 3 components, as shown in (2): semiconductor loss, core loss, and resistive loss, which are evaluated at the points of interest in the EM drive cycle.

$$P_l = P_s + P_c + P_r \tag{2}$$

The designs must also obey a set of 18 design constraints to ensure feasible designs. 17 of the design constraints used in the current study are adopted from [18], which relate to limitations based on geometry, material

considerations, windings, and the objective functions. One constraint is added for the geometrical aspect ratio of the machine to tailor the design for an electrified fluid power system. For the current research, the aspect ratio of the EM is kept to be unity, and the allowable number of pole pairs is kept between 2 and 8.

The design specifications for the EM are carefully considered for the problem at hand. The battery voltage is an important consideration since it affects not only the EM design, but also the choice for battery and inverter architecture. An analysis, on the impact of battery voltage choice for mobile hydraulic applications, in terms of EM performance, was conducted by the authors lab in [24]. This study demonstrated that the EM efficiency is not significantly affected by the battery voltage choice, and an EM designed with a battery voltage of 700 V is slightly more compact than an EM with battery voltage of 96 V. However, a lower voltage rating would imply a higher current, as is the case with 96 V, implying that the losses in the inverter would be higher, as confirmed by [24]. Since the current study is interested in exploring the most optimum scenario in terms of EM size and efficiency, a battery voltage of 700 V is assumed while designing the EM.

Another important aspect to consider is the thermal management of the EM, and the associated winding current densities. Ponomarev [25] and Nishanth [26] provide the ranges of acceptable temperature limits for EMs, and the corresponding combinations of cooling technologies and current density limits that can ensure that these temperature limits are followed. Based on these works, it is assumed that the winding temperature limit is set to 150°C, and the current density limits are set to a conservative value of 20 A-mm^{-2}. It is assumed that the cooling technology during operation is chosen such that the winding material with a current density limit of 20 A-mm^{-2} will stay below 150°C during sustained operation. Furthermore, this constraint on operating current density is employed only for points that are required to operate continuously, and this assumption is relaxed when sizing for points with overload operation. Since current density limits and winding size are inversely correlated, decreasing the allowable current density limits can result in much bulkier EMs. This can happen in situations where the cooling technology is less aggressive. The impact of cooling technology on EM size and efficiency has been explored further in Section 5.

Lastly, one more set of specifications to consider is the EM operating torque and speed for analysis. The EM torque (T_{EM}) and speed (n_{EM}) demand can be obtained from the pump pressure (Δp) and flow (Q_p) demand, displacement (V_d) and operating efficiencies (η_v, η_{hm}), as shown

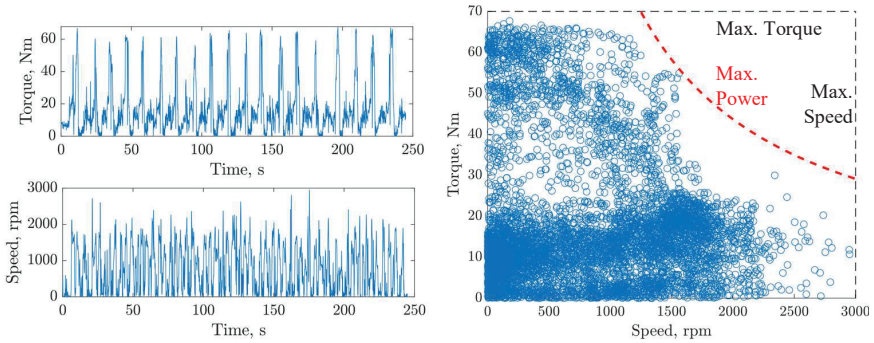

Figure 4 (a) VMFP EM operating demand from the drive cycle, and (b) VMFP EM operating domain.

in (3) and (4)

$$T_{EM} = \frac{V_d \, \Delta p}{\eta_{hm}} \tag{3}$$

$$n_{EM} = \frac{Q_p}{\eta_v \, V_d} \tag{4}$$

The pump efficiency is obtained from experimental data and is fed into the POLYMOD program, developed by Mikeska et al. [27], which interpolates experimental efficiency data and outputs the volumetric, hydromechanical and total efficiencies of the pump as a function of pressure difference speed, and displacement.

For the VMFP ePump architecture, the pump displacement is constant, and the pressure and flow demand of the pump from Figure 3 is converted to EM torque and speed demand, as shown in Figure 4.

In the case of an FMVP architecture, the speed is kept fixed at 3000 RPM, and the displacement is varied according to the pump flow demand. The resulting torque demand for the EM is plotted in Figure 5. As can be seen from (3), the EM operating torque decreases as the pump displacement decreases. This phenomenon, combined with the EM sizing strategies proposed for FMVP, could, in turn, result in highly compact EMs for any given application, which is demonstrated in Section 4.

This paper discusses 3 methods, through which an EM designed for a mobile hydraulic machine can be downsized. These methodologies are:

1. **Changing the ePump architecture:** As can be seen from Figures 4 and 5, the EM sizing torque for an FMVP type ePump is smaller than

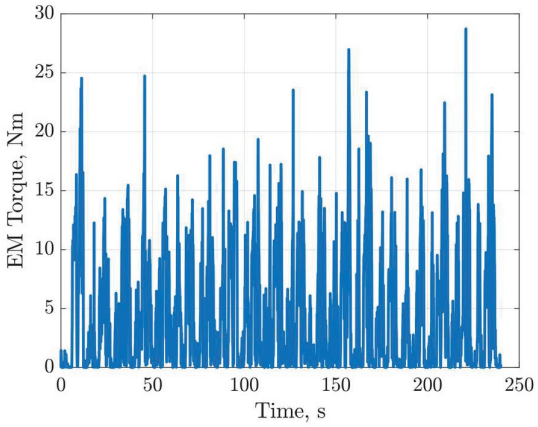

Figure 5 (a) FMVP EM torque demand from the drive cycle.

that for a VMFP type ePump. This represents an opportunity unique to fluid power systems, where downsizing can be achieved by changing the pump type from fixed displacement to variable displacement. The exact impact of changing the ePump type on EM size and efficiency is discussed in Section 4.

2. **Using an operational sizing strategy:** An EM operational sizing strategy is defined as a sizing methodology where points are carefully chosen in the EM operating domain, and EM is designed to operate efficiently at those selected points. This choice of points is often tied to an EM's operational capabilities, like the ability to operate in flux weakening mode or overload mode, and understanding these capabilities is critical to selecting the best operational sizing points. Therefore, Section 3 will further describe the EM operational sizing strategies, as well as the EM torque and speed specifications for each proposed strategy. These operational sizing strategies can also be effectively combined with both VMFP and FMVP ePump architectures. Therefore, Section 3 will describe these operational strategies for both VMFP and FMVP architectures.
3. **Using a better cooling technology:** Increasing the cooling capacity of an EM implies that it can go to higher current densities, implying a possible decrease in EM size. Therefore, Section 5 describes how EM design will change for different cooling technologies. Furthermore, this comparison of cooling technologies is made for each of the operational sizing strategy, and for both ePump architectures.

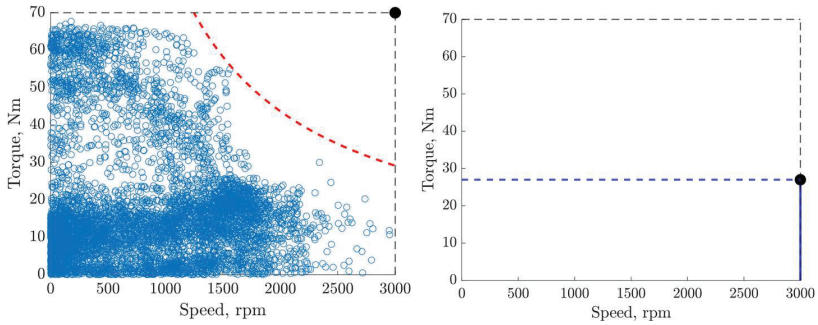

Figure 6 Corner Point sizing points for (a) VMFP and (b) FMVP.

Sections 4 and 5 will demonstrate how each of the independent downsizing methodologies work, how they can be combined effectively, and how do EM size and efficiency trends vary for each methodology. Section 6 will then compare these 3 methodologies in isolation.

3.1 Corner Point operation

In this sizing strategy, a single EM operating point, with the torque and speed value equal to the maximum torque and speed demand of the drive cycle, is used to size the EM. This strategy allows for designing EMs that can provide sustained operation for all combinations of EM torques and speeds below the drive cycle maxima. The location of the sizing point (in black) with respect to the overall operating domain is shown in Figure 6.

For the chosen drive cycle with the VMFP architecture, the maximum torque is 67.67 Nm (rounded up to 70 Nm), and the maximum speed is 3000 RPM.

For the drive cycle with FMVP architecture, owing to the ability to decrease displacement, the maximum torque is 27 Nm, which is lower than the maximum torque for VMFP architecture.

3.2 Flux Weakening Operation

As can be seen from the operating domain, there are no operating points close to the corner point, and the torque requirement for higher speeds is lower. Observation shows that the torque requirement is about 67.67 Nm up to a speed of 1200 RPM. The torque requirement at the maximum speed of 2951 RPM is only about 12 Nm. The point with the maximum power is at a torque equal to 54.6 Nm and a speed equal to 1600 Nm. Therefore, the EM can

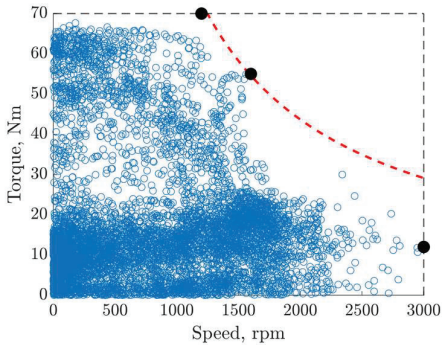

Figure 7 Flux weakening sizing points for VMFP.

be operated in a flux weakening mode for the operating domain with high speed and low torque requirement. The design methodology of PMSMs with flux weakening capability can be found in [8], and research at the authors' lab has demonstrated this strategy for fluid power systems in detail in [9]. Therefore, 3 points are considered for sizing the EM based on maximum torque, maximum speed, and maximum power requirement. These points are shown in Figure 7.

3.3 Current Ratio-based Transient Operation

Looking back at the drive cycle in Figure 4, the highest torque requirement is needed for only short durations, and sustained operation is required for lower torque values. This fact can be leveraged to design EMs that can sustain operation at lower torque values and provide high torques while operating in overload conditions. Therefore, the sizing torque used for the optimization can be reduced based on the chosen overload current ratio. When operating in transient conditions, the constraint on current density is relaxed since the EM operates at those points only for a very short duration, and the current density limit is active only for points with sustained operation.

For the current study, the overload current ratio (CR) is taken as 1.73, as reported by Pellegrino et al. [12]. Therefore, the sizing torque becomes:

$$T_{rated} = \frac{T_{max}}{CR_{overload}} = \frac{T_{max}}{1.73} \tag{5}$$

For the VMFP architecture, the sizing torque comes out to be 39.11 Nm (rounded up to 40 Nm). For the FMVP architecture, the torque comes out to be 15.6 Nm.

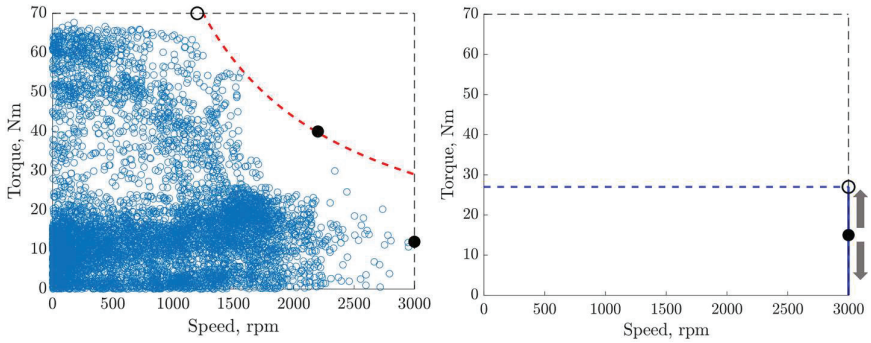

Figure 8 Transient operation sizing points for (a) VMFP and (b) FMVP.

3.4 RMS Torque-based Transient Operation

Another calculation for torque in transient conditions comes in the form of RMS torque calculation, as demonstrated in [14] for on-road vehicles, but can also be incorporated into ORVs. In this case, the sizing torque is calculated as the RMS value of torque during the entire drive cycle.

$$T_{rated} = T_{RMS} = \left(\frac{1}{t_{DC}} \int_0^{t_{DC}} (T_{EM})^2 dt \right)^{\frac{1}{2}} \tag{6}$$

For the 245-second VMFP drive cycle, the value of the sizing torque comes out to be 23.40 Nm (rounded up to 24 Nm), which is about 35% of the maximum torque, similar to the value reported for EMs in on-road vehicles in [14] and is also smaller than the current ratio (CR) based rated torque.

For the FMVP drive cycle, this RMS torque value is 6.5 Nm, which is also much lower than the CR-based sizing for FMVP and is equal to 24% of max torque.

The transient operation points are shown in Figure 8.

3.5 EM Optimization

The genetic algorithm-based optimization for the PMSMs is built using the above specifications, and the optimization is run till convergence. The formal mathematical problem definition for the EM optimization is included in Table 1 for completeness, however, readers are encouraged to refer to [18] for the detailed derivation of the EM parametrization and design constraints mentioned here.

Table 1 EM optimization problem statement

Objectives:	$\min(S_{EM})$ $\min\left(\sum_i P_{l,EM}(T_{e,i}, \omega_{rm,i})\right)$ where, $[T_{e,i}, \omega_{rm,i}]$: EM torque and speed at the sizing point
By varying:	$\theta = [S\ R\ C\ M\ \boldsymbol{G_I}\ \boldsymbol{W_I}\ \boldsymbol{I_I}]$ where, $[S,\ R,\ C,\ M]$: Material properties for stator, rotor, conductor and magnets $\boldsymbol{G_I}$: Geometry parameters $\boldsymbol{W_I}$: Winding parameters $\boldsymbol{I_I}$: Operation Currents
Subject to constraints:	1. Tooth aspect ratio must be within a pre-determined range 2. Wire diameter must be smaller than stator slot width 3. Current density must be within limits: $\frac{I_s}{a_c} \leq J_{\text{lim}}$ 4. EM mass must be within limits: $M_{EM} \leq M_{\text{lim}}$ 5. Peak line-to-line voltage less than DC link voltage: $v_{ll,pk} \leq v_{DC} - 2v_{fs}$ 6. The stator and rotor must not be saturated at 0 current. 7. The stator and rotor must not be saturated at operating current. 8. Required torque must be achieved: $T_{operating} \geq T_{e,i} - \frac{P_{c,i}}{\omega_{rm,i}}$ 9. EM operating power loss must be within limits: $P_{l,EM} \leq P_{l,EM,\text{lim}}$ 10. Aspect ratio $= \frac{d_{EM}}{L_{EM}} = 1$

This optimization compares the trade-offs between size and aggregate power loss and generates Pareto designs with the two fitness functions, as shown in Figure 9. Each point in the Pareto front represents one specific design generated by the optimization algorithm. One of the main benefits

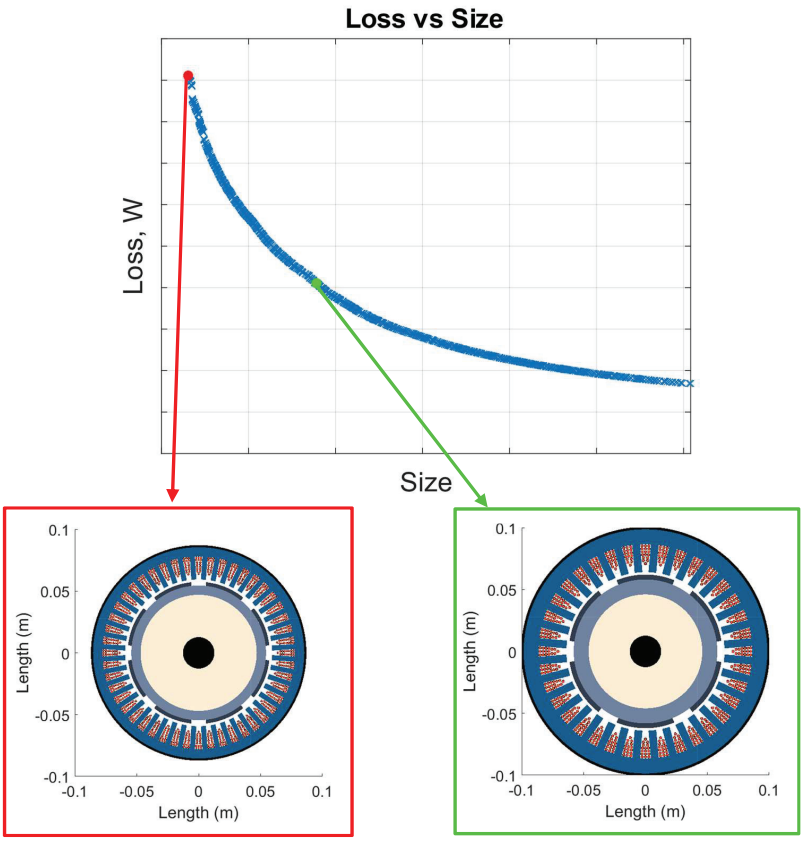

Figure 9 Pareto front and corresponding EMs generated from the optimization procedure.

of the proposed operational sizing strategies is in producing highly compact designs. Therefore, the most compact design from the Pareto front (highlighted in red) of each optimization is chosen for size and efficiency comparison purposes. However, more efficient but less compact designs (like the one shown in green) can also be selected for each case, in which case a comparison of only efficiencies can be made.

4 Electric Machine Design Results

This section describes the designs generated by the EM optimization, incorporating all the operational sizing strategies discussed in the previous section.

4.1 Comparison of EM Size

The trends for the EM size, mass, and volume generated through optimization for each strategy can be observed in Figures 10, 11, and 12, respectively. The results are in the format of a bar chart, where the x-axis represents the quantity being compared and the y-axis represents the operational sizing strategies. The EM sizes for the two ePump architectures, VMFP and FMVP are plotted separately, but with a common x-axis for easy interpretation.

Several observations can be made from the comparison chart:

1. As expected, the corner point sizing for VMFP produces the bulkiest EM for a given application.
2. In the case of VMFP, the flux weakening-based EM is smaller than the corner point-sized EM, and the transient operation-based EM is more compact than both.
3. Among the transient-based EMs, the EM sized with the RMS torque approach is more compact than the CR-based EM. This trend results from high dynamics in the case of a mobile hydraulic application, where the RMS torque is much lower than max torque.
4. For each operational sizing strategy, the EMs designed for the FMVP architectures are more compact than the EMs in VMFP architecture.

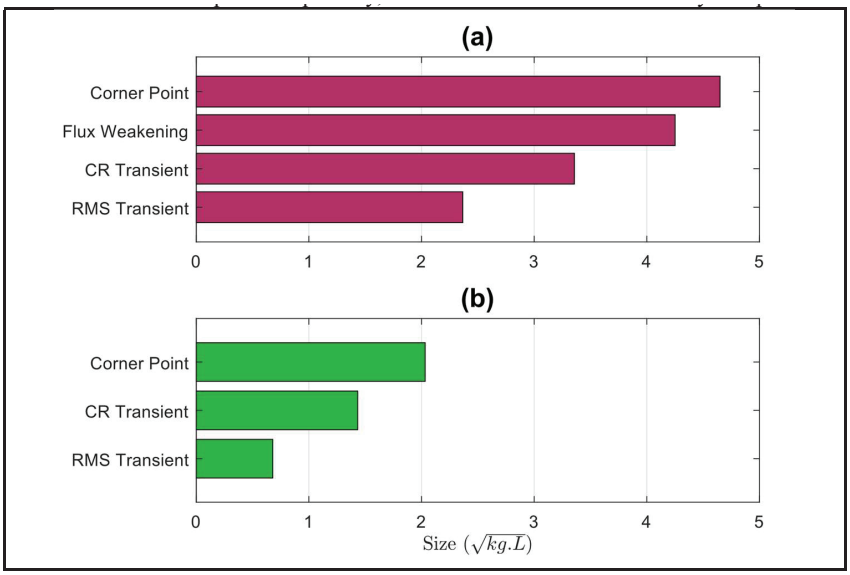

Figure 10 Size comparison among operational strategies for (a) VMFP and (b) FMVP.

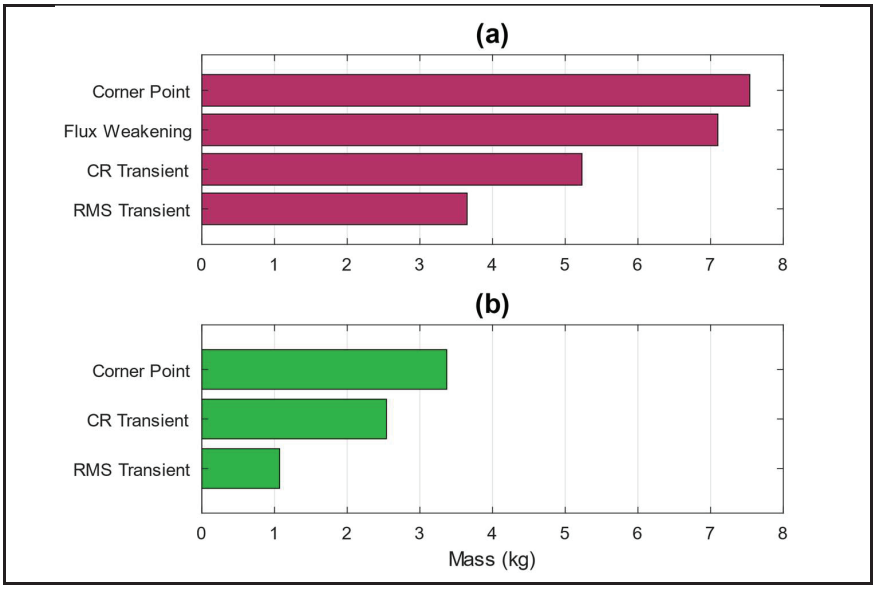

Figure 11 Mass comparison among operational strategies for (a) VMFP and (b) FMVP.

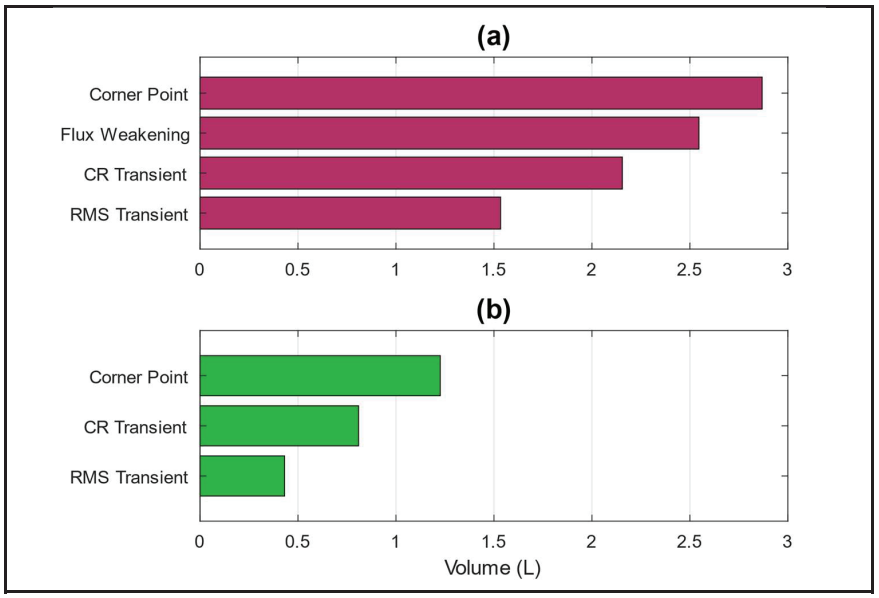

Figure 12 Volume comparison among operational strategies for (a) VMFP and (b) FMVP.

This can be attributed to the lower value of sizing torque in the case of FMVP architecture

5. The trend for EM size in FMVP sizing technology, corner point sizing, and transient sizing is the same as VMFP, implying that these operational sizing strategies can be combined for either ePump architecture with similar benefits.

4.2 Comparison of EM Efficiency

For the calculation of the aggregate drive cycle EM efficiency, the efficiency map is treated as a lookup table $(LT(T, \omega))$ to extract instantaneous power loss based on the drive cycle. This power loss is integrated to find the energy loss over the entire drive cycle, which, when divided by energy input, yields the aggregate energy efficiency of the EM.

$$\eta_{power,EM}(t) = LT(T(t), \omega(t)) \tag{7}$$

$$\eta_{DC,EM} = \frac{\int_0^{t_{DC}} [\eta_{power,EM}(t) \cdot T(t) \cdot \omega(t)] dt}{\int_0^{t_{DC}} [T(t) \cdot \omega(t)]\, dt} \tag{8}$$

The trends for the cycle efficiency of each EM strategy can be seen in Figure 13.

The following conclusions can be drawn from the efficiency trends:

1. The EM efficiency for FMVP architectures is higher than for VMFP. This could be attributed to the high-speed operation in the case of FMVP. Note that this efficiency calculation does not consider HM efficiency.
2. The sizing with flux-weakening does not significantly affect the EM efficiency and, in fact, improves it. This could be attributed to the EM generated through flux weakening strategy operating in a high-efficiency region.
3. The sizing with the transient operation of EM is lower due to the EM operating above rated limits for some parts of the drive cycle. Among the 2 cases with transient operation, the EM sized with RMS torque particularly experiences a significant drop in efficiency.

The radial cross-sections for the Electric Machines designed from each optimization are also useful, as they can provide information regarding winding configuration and pole pairs for the EMs generated in each case. Therefore, the radial cross-sections of one quarter of the designed EMs for the current case are shown in Figure 14. The axes represent length in metres.

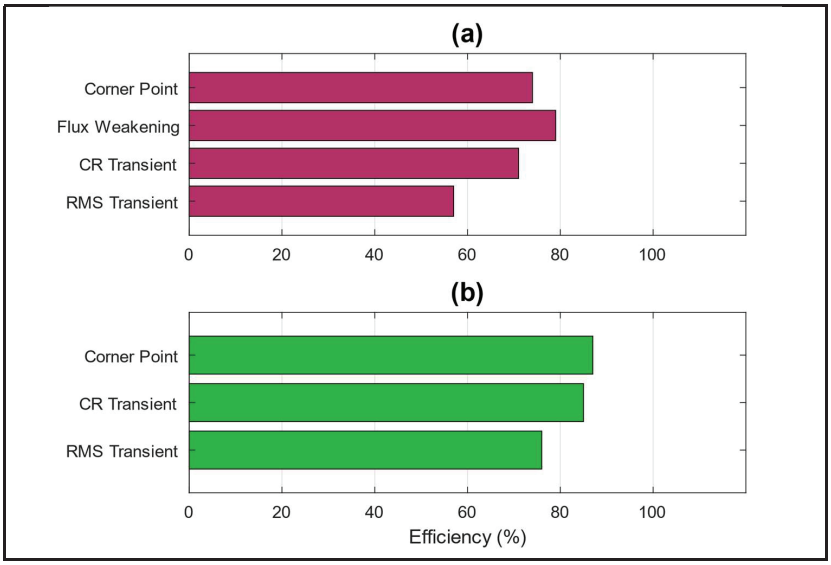

Figure 13 Efficiency comparison for operational strategies for (a) VMFP and (b) FMVP.

5 Effect of Cooling Technology

The design specifications presented in previous sections had assumed that the maximum current density in the EM windings during sustained operation must be less than 20 A-mm^{-2}. This constraint ensures that the EM windings are not damaged due to heating. It is known that the resistive power loss in conductors is given by (9).

$$P_{resistive} = I_s^2 R = \frac{J \times I_s \times l}{\sigma} \tag{9}$$

Using aggressive cooling technology, like immersion cooling for stator windings, can ensure that current densities of 20 A-mm^{-2} or lower can ensure a maximum winding temperature limit of 150°C. However, in case of a less aggressive cooling strategy, like air cooling or use of water jackets, high current densities could result in high winding temperatures. Therefore, it might be necessary to constrain the current density to a lower value. The current density range for each cooling strategy can be seen in Table 2 [25].

Therefore, it becomes important to observe the effect of EM sizing strategies when the cooling technology is changed. To incorporate this, the EM optimization tool used in the previous sections is modified with the current density constrained to a maximum of 10 A-mm^{-2} while keeping all

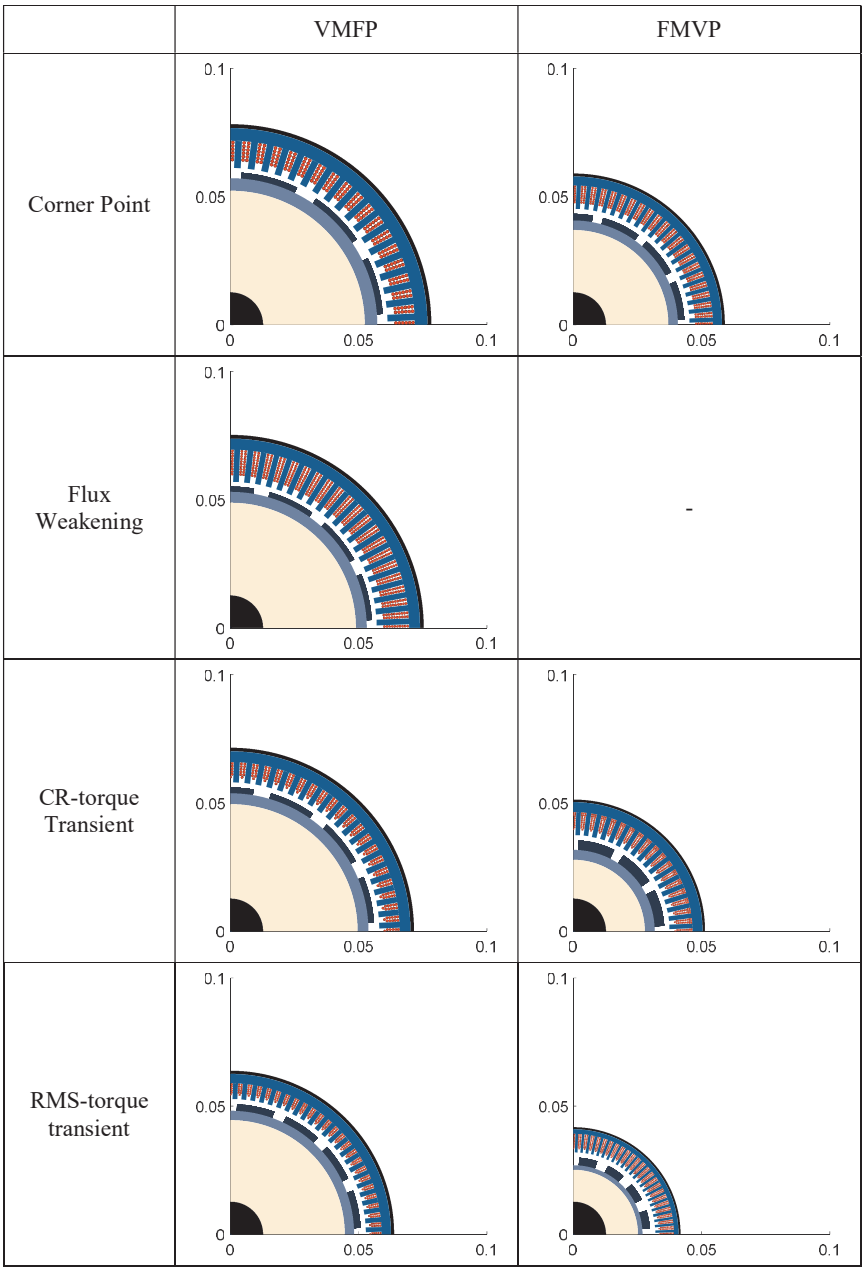

Figure 14 Radial Cross-sections for EM designs for each sizing strategy.

Table 2 EM Winding current density limit corresponding to each cooling technology

Thermal Management Strategy	Current Density Range (A-mm^{-2})
Convective air cooling	2–4
Forced air cooling	4–8
Water stator jacket	6–14
Direct in-wire armature cooling	10–25
Direct immersion and spray cooling	8–28

other design parameters the same, and the optimization is run for all sizing strategies till convergence. The results are shown in following subsections.

5.1 Change in EM Size and Efficiency by Switching Cooling Constraint

The size, mass, and volume comparisons between sizing strategies for both current densities are shown in Figures 16–18, respectively, following the plotting convention in Section 4. The following conclusions can be drawn from Figures 15–17:

1. When the allowable current densities are much lower, the designed EMs are bulkier, and this holds for all sizing strategies.
2. For the sizing strategies, for the case with $J \leq 10$ A-mm^{-2}, the size follows the same trend as in the case of $J \leq 20$ A-mm^{-2}.

The efficiencies for the EMs designed is shown in Figure 18, and it can be concluded that:

1. The efficiency trend for the operational sizing strategies is the same for both current density limits. This implies that the effectiveness of the operational sizing strategies, in terms of EM efficiency, does not depend on the current density limit.
2. The efficiency of EMs with lower current density limits is higher than before. This is expected as the resistive losses decrease with a decrease in operating current density, thus increasing efficiency.

The radial cross-section of the new EMs is shown in Figure 19, with comparison done in 2 separate tables, one for each ePump architecture.

Upon comparison between the 2 sets of the EMs (left-side EMs with lower cooling constraints and right-side EMs with higher cooling constraints), an interesting observation can be made: the number of rotor magnets (and hence the poles) for the optimal EM increases when the cooling technology is improved. This can be an important consideration when choosing

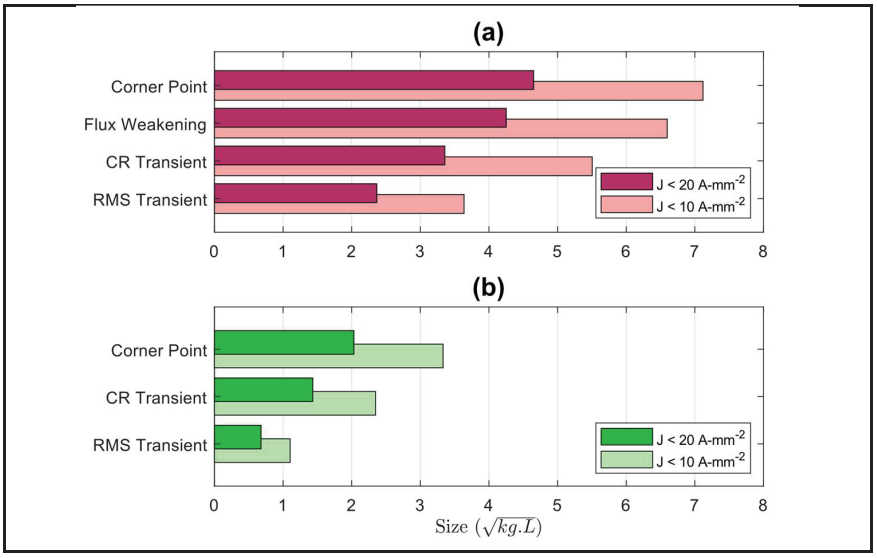

Figure 15 EM Sizes for different cooling constraints for (a) VMFP and (b) FMVP.

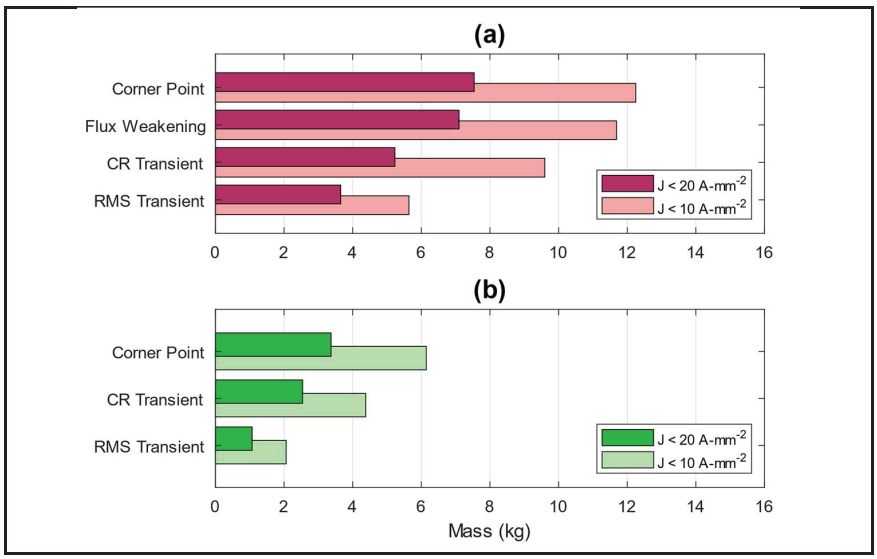

Figure 16 EM Masses for different cooling constraints for (a) VMFP and (b) FMVP.

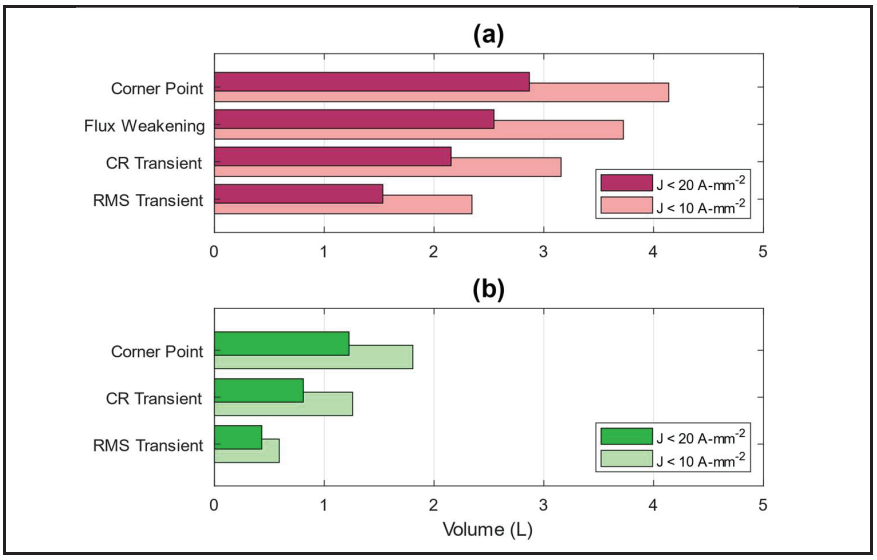

Figure 17 EM Volumes for different cooling constraints for (a) VMFP and (b) FMVP

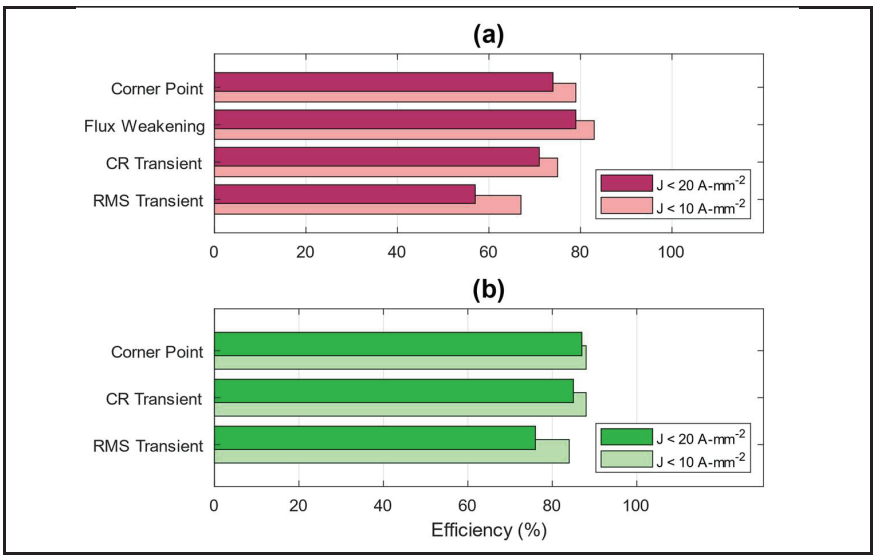

Figure 18 EM Efficiencies for different cooling constraints for (a) VMFP and (b) FMVP.

A	VMFP	
	J = 10 A-mm^{-2}	J = 20 A-mm^{-2}
Corner Point	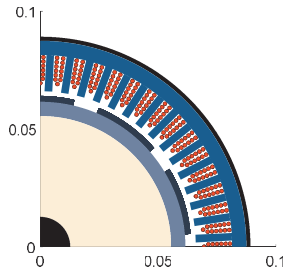	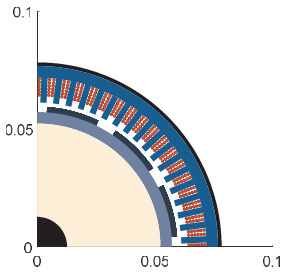
Flux Weakening	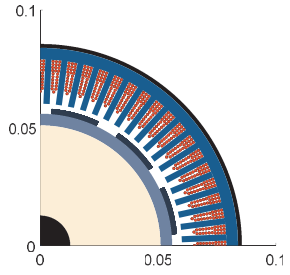	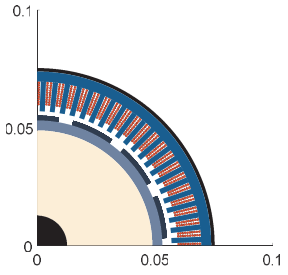
CR-torque Transient	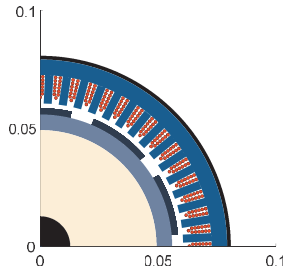	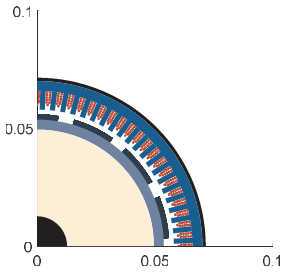
RMS-torque transient	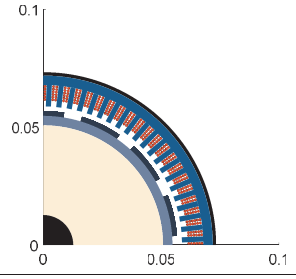	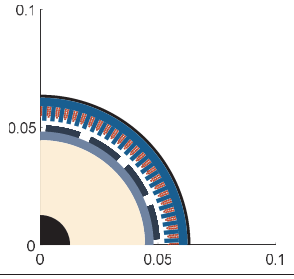

Figure 19 Continued

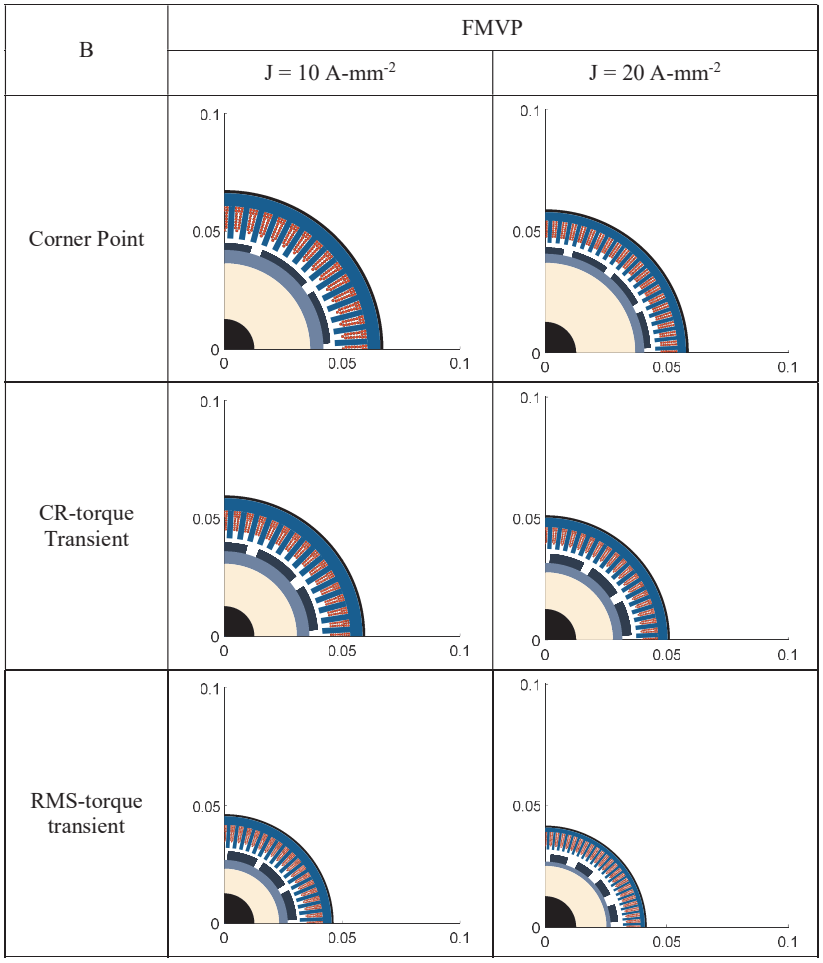

Figure 19 (A) Radial Cross-sections for EM designs with new cooling constraint for VMFP. (B) Radial Cross-sections for EM designs with new cooling constraint for FMVP.

the cooling technology, since magnets may account for a large portion of an EM's cost

5.2 Trends in EM Size for Multiple Cooling Constraints

To further study the mutual interaction between the two downsizing methods, (i) using a proposed operational sizing strategy and (ii) using an improved cooling technology, EMs were designed with multiple different cooling

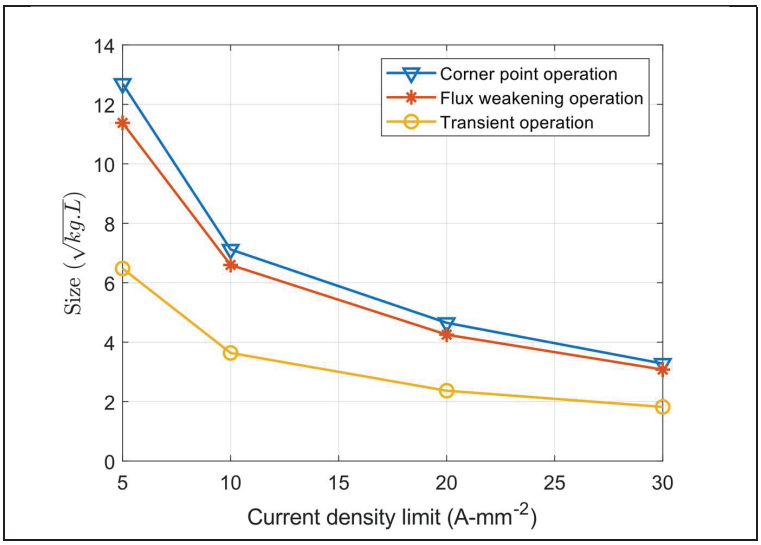

Figure 20 EM Size vs current density limits for different operational sizing strategies.

constraints and the current density limit range from Table 1 for each operational sizing strategy, with VMFP ePump architecture. The resulting plot in Figure 20 shows the EM size vs current density limit for corner point operation, flux weakening operation, and transient operation. Each point in the plot represents an EM designed through optimization.

The following inferences can be made from Figure 20:

1. The improvement in EM size gives diminishing results for higher current density limits for all operational sizing strategies. This implies that further improving the cooling technology provides a minimal benefit if the current density limits are already high.
2. The improvement in EM size for each operational sizing strategy is the same for all current density limits. This implies that the operational sizing strategies can be useful, irrespective of the cooling technology used, and they can be combined with cooling improvements to downsize EMs effectively.

6 Comparison of Downsizing Methodologies

Three methods have been discussed in this paper so far for downsizing electric machines. Those methods are (i) Switching the ePump architecture,

Table 3 Design aspects of 5 chosen EMs to compare downsizing methods

Design Aspect/No.	J_{lim} Based on a Cooling Technology (A-mm^{-2})	Operational Sizing Strategy	ePump Architecture
A (Baseline)	10	Corner Point	VMFP
B	10	**Flux Weakening**	VMFP
C	**20**	Corner Point	VMFP
D	10	**RMS Transient**	VMFP
E	10	Corner Point	**FMVP**

(ii) Switching the cooling technology to improve current density limits, and (iii) Using one of the operational sizing strategies. Each of these methods and their combinations can be used to obtain a compact EM, as described in Sections 4 and 5. However, it is also worth comparing these three methodologies in isolation to observe their individual effectiveness. Therefore, five specific designs are chosen, as shown in Table 3, where only one design aspect for each design is changed (highlighted in red) from the baseline design A, and these designs are then compared.

The five designs are compared in a radial plot in Figure 21. The axes for EM size, EM mass and EM volume, denoted by (S_{EM}), (M_{EM}), (V_{EM}), clock-wise have been normalized with respect to the Baseline design 'A', on a scale of 0–1. The fourth axis $(1 - \eta_{EM})$ is an indication of the non-dimensionalized EM power loss for a drive cycle on a scale of 0–1. Since it is desirable that all 4 of these parameters be minimized for an EM, the area enclosed in the radial plot for any curve is an indicator of how effective a particular design is.

From the comparison, it can be seen that the most effective method for EM downsizing is to switch the ePump architecture, followed by using an operational sizing strategy (specifically based on RMS torque transient operation) and improving the current density limit through better cooling being the least effective option in this case. However, it is possible to switch this trend by using a different operational sizing strategy (like flux weakening, as shown) or by improving the cooling performance by a larger amount than shown here.

Furthermore, the EM efficiency in each case (B–E) is very close to the baseline design A, and as demonstrated in previous sections, changing the ePump architecture can improve the efficiency, while using an aggressive cooling technology with higher current densities can decrease it.

Therefore, switching to FMVP ePumps and using aggressive EM cooling technology are both very attractive options that can be used for designing

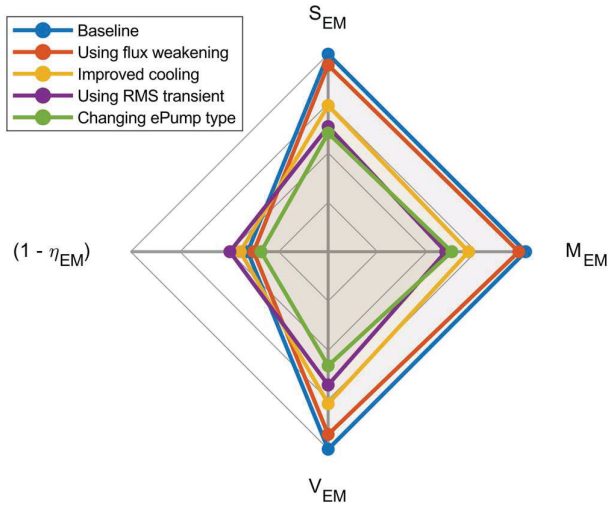

Figure 21 EM size comparison based on different downsizing methods.

compact EMs in fluid power applications. However, these options can typically involve additional costs and system design considerations, and it may even be impossible to pursue these options in specific situations. However, from Figure 21, it is evident that the operational sizing strategies can give just as much benefit as the other two downsizing methods in terms of EM size. As demonstrated in Sections 4 and 5, these operational sizing strategies can be used effectively for any cooling constraint or ePump architecture, and their implementation does not involve any additional costs.

7 Scope and Limitations

This paper proposes operational sizing strategies that can be used when sizing an EM for an electrified mobile hydraulic application. A reference case, of a mini-excavator's arm actuator has been considered for analysis. The paper shows trends in EM size based on 2 different ePump architectures, different operational sizing strategies, and different cooling technologies. This analysis has very wide applications, in that the fundamental operational sizing strategies can be used with any actuator, and any machine. Since the trends of the operational sizing strategies are based on EM operational capabilities and EM morphology, instead of drive cycles, many of the trends shown here will still hold. This analysis can be extended in the future, to study overrunning loads, like in the boom actuator, or a system with lesser dynamics, like

an agricultural application, to study how the EM size and efficiency trends evolve. This analysis can also be further conducted for shaftless integrated EHUs, where compactness is an even bigger consideration, but there are additional thermal and geometric constraints involved, which can affect how effective each of these operational strategies are.

However, the reader must be cautious when studying these trends. The exact values of size and efficiency depend heavily on the actuator and drive cycle being considered, and therefore, this analysis must be treated as a basis, and must be conducted again for a different specific application. The current study does not cover any considerations on costs, sustainability or maintenance, since these parameters can often be highly subjective, and the user must take these additional considerations into account when designing the entire electric system of the machine. Lastly, this study focuses primarily on the EM design, without making any comments on the exact choice methodology for battery, inverters, motor controller, and additional system integration components like hoses, fittings, cables, etc., which are out of scope for this study. The trends shown in this paper are independent of such choices, however the user must size these components for their specific application, such that their operating requirements are met.

8 Conclusions

This paper proposes and compares operational sizing strategies that can be used to design an EM for any electrified mobile hydraulic application and presents the design procedure for a reference application. The resulting EMs show that these strategies can be used to design significantly more compact EMs without a considerable impact on EM operational efficiency. This makes these strategies particularly well-positioned to be applied to mobile hydraulic applications, where the low power density of existing EMs hinders their widespread adoption. To take this analysis further, the strategies are analysed, combined with other well-known methods to downsize EMs: using variable displacement pumps and better cooling technology. The comparison shows that these operational sizing strategies can be effectively used for any ePump architecture and cooling technology to yield a considerable benefit in downsizing EMs. The paper also showed that when used in isolation, these operational sizing strategies give as much benefit as the other two mentioned methods without the overhead of additional costs or system-level modifications. The strategies, specifically related to the EM overload operation, can be studied further in-depth, by incorporating a more well-rounded thermal

analysis. The implementation of the current-ratio based overload and RMS torque-based overload operation have been adopted directly from on-road vehicles, and their exact formulation must be studied/modified for fluid power applications. The current study considers surface-mounted PMSMs, however, a similar analysis can be conducted for other PMSM topologies, since these can differ in terms of overload capacity. These strategies can be further extended for actuators with overrunning loads, like an excavator's boom, and can also consider a VMVP ePump architecture. In any case, the proposed strategies have immense potential in bridging the gap between the power densities of hydraulic and electric machines and accelerating the adoption of EMs for mobile hydraulic applications.

References

[1] S. Sakama, Y. Tanaka, and A. Kamimura, "Characteristics of Hydraulic and Electric Servo Motors," *Actuators*, vol. 11, no. 11, pp. 1–18, 2022.

[2] B. J. Chalmers, E. Spooner, O. Honorati, F. Crescimbini, and F. Caricchi, "Compact permanent-magnet machines," *Electr. Mach. Power Syst.*, vol. 25, no. 6, pp. 635–648, Jul. 1997.

[3] T. Finken, M. Felden, and K. Hameyer, "Comparison and design of different electrical machine types regarding their applicability in hybrid electrical vehicles," in *Proceedings of the 2008 International Conference on Electrical Machines, ICEM'08*, 2008, pp. 1–5.

[4] F. N. U. Nishanth, G. Bohach, J. Van De Ven, and E. L. Severson, "Design of a Highly Integrated Electric-Hydraulic Machine for Electrifying Off-Highway Vehicles," *2019 IEEE Energy Convers. Congr. Expo. ECCE 2019*, pp. 3983–3990, 2019.

[5] T. Wang and Q. Wang, "Coupling effects of a novel integrated electro-hydraulic energy conversion unit," *Int. J. Appl. Electromagn. Mech.*, vol. 47, no. 1, pp. 153–162, 2015.

[6] T. Pietrzyk, D. Roth, G. Jacobs, and S. Katharina, "Design of a high speed internal gear pump to increase the power density of electro hydraulic actuators (EHA) in mobile applications," in *ASME International Mechanical Engineering Congress and Exposition, Proceedings (IMECE)*, 2019, vol. 7, pp. 1–9.

[7] Puranen J. Induction motor versus permanent magnet synchronous motor in motion control applications: a comparative study. PhD. Thesis, Lappeenranta University of Technology, Lappeenranta, Finland, 2006.

[8] S. D. Sudhoff, K. A. Corzine, and H. J. Hegner, "A Flux Weakening Strategy for Current-Regulated Surface-Mounted Permanent-Magnet Machine Drives," *IEEE Trans. Energy Convers.*, vol. 10, no. 3, pp. 431–437, 1995.

[9] S. Sarode, L. Shang, A. Vacca, and S. D. Sudhoff, "Flux Weakening Operation Based Design of an Integrated Electrohydraulic Axial Piston Unit," in *Proceedings of the BATH/ASME 2022 Symposium on Fluid Power and Motion Control*, 2022.

[10] T. A. Minav, J. J. Pyrhönen, and L. I. E. Laurila, "Permanent magnet synchronous machine sizing: Effect on the energy efficiency of an electro-hydraulic forklift," *IEEE Trans. Ind. Electron.*, vol. 59, no. 6, pp. 2466–2474, 2012.

[11] F. Zappaterra, A. Vacca, and S. D. Sudhoff, "A compact design for an electric driven hydraulic gear machine capable of multiple quadrant operation," *Mech. Mach. Theory*, vol. 177, pp. 1–31, Nov. 2022.

[12] G. Pellegrino, A. Vagati, P. Guglielmi, and B. Boazzo, "Performance comparison between surface-mounted and interior PM motor drives for electric vehicle application," *IEEE Trans. Ind. Electron.*, vol. 59, no. 2, pp. 803–811, 2012.

[13] Parker Hannifin, "GVM142 Global Vehicle Motor Generators for Vehicle Applications.", GVM142_Electric_Motor_Catalog_NA.pdf (parker.com)

[14] M. Gamba, "Design of non conventional Synchronous Reluctance machine," Politecnico di Torino, 2017.

[15] R. Rahmfeld and M. Ivantysynova, "Energy saving hydraulic actuators for mobile machines," *1st Bratislavian FLUID POWER Symp.*, vol. 49, no. 203, pp. 1–11, 1998.

[16] S. Kärnell, "Fluid Power Pumps and the Electrification in Load Handling Applications," Linköping Studies in Science and Technology, 2020.

[17] Assaf H, Sarode S, Vacca A, Sudhoff SD. Electric machine sizing consideration for ePumps in mobile hydraulics. Energy Sci Eng. 2023;1-17. doi:10.1002/ese3.1654.

[18] S. D. Sudhoff, *Power Magnetic Devices: A Multi-Objective Design Approach, Second Edition*. 2021.

[19] S. D. Sudhoff, "Genetic Optimization System Engineering Tool." 2014.

[20] Sarode, Shanmukh, Assaf, Hassan, Shang, Lizhi, Vacca, Andrea, Sudhoff, Scott. (2023). Optimizing Electric Machines for Off-road Mobile Applications.

[21] E. Busquets and M. Ivantysynova, "A Multi-Actuator Displacement-Controlled System with Pump Switching–: A Study of the Architecture and Actuator-Level Control," *JFPS Int. J. Fluid Power Syst.*, vol. 8, no. 2, pp. 66–75, 2014.

[22] Zimmerman, Joshua & Busquets, Enrique & Ivantysynova, Monika. (2011). 40% Fuel Savings by Displacement Control Leads to Lower Working Temperatures – A Simulation Study and Measurements.

[23] Casoli P, Scolari F, Minav T, Rundo M. Comparative Energy Analysis of a Load Sensing System and a Zonal Hydraulics for a 9-Tonne Excavator. Actuators. 2020; 9(2):39. https://doi.org/10.3390/act9020039.

[24] Sarode S, Shang L, Vacca A, Sudhoff S. Design methodology for an integrated axial piston-type electrohydraulic unit. Proceedings of the Institution of Mechanical Engineers, Part C: Journal of Mechanical Engineering Science. 2024;238(5):1218–1233. doi: 10.1177/09544062231185517.

[25] P. Ponomarev, "Tooth-Coil Permanent Magnet Synchronous Machine Design for Special Applications," Lappeenranta University of Technology Finland, 2013.

[26] F. Nishanth, M. Johnson and E. L. Severson, "A Review of Thermal Analysis and Management of Power Dense Electric Machines," 2021 IEEE International Electric Machines & Drives Conference (IEMDC), Hartford, CT, USA, 2021, pp. 1–8, doi: 10.1109/IEMDC47953.2021.9449520.

[27] D. Mikeska, and M. Ivantysynova. "A precise steady-state model of displacement machines for the application in virtual prototyping of power-split drives." In Proceedings of the 2nd International FPNI-PhD Symposium on Fluid Power, Modena, Italy, pp. 3–6. 2002.

Biographies

Parth Tawarawala received his bachelor's degree (B. Tech) in Mechanical Engineering from Indian Institute of Technology (IIT) Bombay, India in 2022. He is currently a PhD student in Mechanical Engineering and a graduate research assistant at the Maha Fluid Power Research Center, Purdue University. His research areas include design and modelling of hydrostatic pumps, electrohydraulic system design and electrification.

Shanmukh Sarode received his bachelor's degree (B. Tech) in Mechanical Engineering from Sardar Vallabhbhai National Institute of Technology, Surat, India in 2017, the MS in Mechanical Engineering in 2021, and a PhD in Mechanical Engineering from Purdue University in 2023, respectively. He is currently working as an Engineer at Parker Hannifin Corporation at the Motion Technology Center, Cleveland, OH, USA. His research areas include modelling of hydrostatic and hydrodynamic pumps, electrohydraulic system design, and electrification.

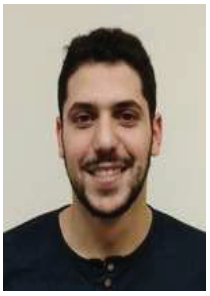

Hassan Assaf received the bachelor's and master's degree in Mechatronic Engineering from Polytechnic University of Turin, and a PhD in Agricultural and Biological Engineering from Purdue University in 2023, respectively. He is currently working as a Senior Systems Engineer at Caterpillar Inc., Peoria, IL, USA. His research areas include electrohydraulic actuation design, fluid power education, and fluid power systems.

Andrea Vacca is the Maha Fluid Power Faculty Chair and a Professor at Purdue University. He currently leads the Maha Fluid Power Research Center which was established in 2004 by the late Prof. Monika Ivantysynova. Dr. Vacca completed his studies in Italy (Ph.D. from the University of Florence in 2005), and he joined Purdue University in 2010 after being an Assistant Professor at the University of Parma (Italy). Fluid power technology has been Dr. Vacca's major research interest since 2002. Dr. Vacca authored the textbook "Hydraulic Fluid Power" by Wiley and more than 150 technical papers, most of them published in international journals or referred conferences. He is chair of Fluid Power Systems and Technology Division (FPST) of the American Society of Mechanical Engineers (ASME), and a former chair of the Fluid Power Division of the Society of Automotive

Engineers (SAE). Dr. Vacca is also one of the Directors of the Global Fluid Power Society (GFPS). Furthermore, he is also the Editor in Chief of the International Journal of Fluid Power. Dr. Vacca also received the 2019 J. Bramah medal of the Institution of the Mechanical Engineers (IMechE).

Lizhi Shang earned his Ph.D. from Purdue University in 2018 with the guidance of his Ph.D. advisor, the late Dr. Monika Ivantysynova. His dissertation focuses on the scaling of the axial piston machine lubricating interfaces. Dr. Shang joined Purdue University as an assistant professor in 2020. Since then, he has led a research group at the Maha fluid power research center studying designing and modelling hydrostatic pumps and motors, hydrodynamic pumps and turbines, fluid power systems, and advanced computational and experimental tribological analysis. His research aims to improve the energy efficiency, reliability, and controllability of fluid power systems by conducting interdisciplinary research on both component and system levels and exploring and expanding fluid power's use and fluid power technology in new applications.

Scott D. Sudhoff (Fellow, IEEE) received the B.S. (Hons.), M.S., and Ph.D. degrees in electrical engineering from Purdue University, West Lafayette,

IN, USA, in 1988, 1989, and 1991, respectively. From 1991 to 1993, he worked as a Consultant at P. C. Krause and Associates in aerospace power and actuation systems. From 1993 to 1997, he was also a Faculty Member with the University of Missouri–Rolla. In 1997, he joined as a Faculty Member with Purdue University, where he is currently the Michael and Katherine Birck Professor of electrical and computer engineering. His research interests include electric machinery, power electronics, marine and aerospace power systems, applied control, evolutionary computing, and genetic algorithms and their application to power electronic converters and electric machine design. He has published over 200 papers in these areas, including six prize papers. He served as the Editor-in-Chief for IEEE Transactions on Energy Conversion and IEEE Power and Energy Technology System.